bulk solids handling Volume 6, Number 4, August 1986

Wall Pressure-Feeder Load Interactions in Mass Flow Hopper/Feeder Combinations

Part I

K.S. Manjunath and A.W. Roberts, Australia

Abstract

The interactive roles of mass flow bins and feeders are discussed. The effect of feeder speed, gate height, clearance between the hopper outlet and the feeder surface, method of filling, rate of filling on wall pressures in mass flow bins and feeder load and power requirements of the feeders are highlighted. Measurement of wall pressures suggests that initial pressures during filling are less than hydrostatic, hence initial loads on feeders are less than theoretically predicted. The higher experimental flow loads on the feeders are due to the fact that the measured values of wall pressures towards the vicinity of the outlet of the hopper diverge from the radial stress field theory of Jenike. On the basis of the above measurements, the values of K and n are computed and the bounds for initial filling are suggested. The flow loads are based on the major consolidating stress σ_1, which compares satisfactorily with the measured values. Finally, methods to control overloading of the feeders are discussed.

Nomenclature

- a — gate height
- A — area
- B — hopper opening dimension and width between skirtplates
- B_b — belt width
- c — clearance between hopper and feeder
- D — bin diameter or width
- ff — flow factor
- F_a — force to accelerate material onto belt
- F_b — empty belt resistance
- F_{be} — belt load resistance, extended section beyond hopper
- F_{bh} — belt load resistance, hopper section
- F_f — tangential force, flow condition
- F_i — tangential force, initial condition
- F_s — skirtplate friction
- F_{spe} — skirtplate resistance, extended section beyond hopper
- F_{sph} — skirtplate resistance, hopper section
- g — acceleration due to gravity
- h_c — surcharge head acting at transition of cylinder and hopper
- h_o — distance from apex to transition of hopper
- h_s — bin surcharge head
- H — head of bulk solid in cylinder
- H_h — height of hopper
- H_s — actual bin surcharge
- K — ratio of p_n/p_v for hopper
- K_j — pressure ratio in Janssen equation
- K_v — ratio of lateral to vertical pressure in skirtplate zone
- L — length of slotted hopper opening in plane flow bin
- L_c — length of conveyor
- L_s — length of skirtplates
- m — hopper shape factor; $m = 1$ for axisymmetric hopper, $m = 0$ for plane flow hopper
- m_c — cylinder shape factor; $m_c = 1$ for square or circular cylinder, $m_c = 0$ for rectangular cylinder
- m_s — surcharge factor; $m_s = 1$ for conical surcharge, $m_s = 0$ for triangular surcharge
- n — factor of index in bin pressure distribution equation
- p_n — normal wall pressure
- p_v — average vertical pressure
- P — power
- q — nondimensional surcharge factor
- q_f — nondimensional surcharge factor, flow condition
- $q_{f\sigma_1}$ — nondimensional flow surcharge factor based on σ_1
- q_i — nondimensional surcharge factor, initial condition
- Q — feeder load
- Q_f — feeder load, flow condition
- $Q_{f\sigma_1}$ — feeder load based on σ_1
- Q_i — feeder load, initial condition
- R — hydraulic radius
- v — belt velocity
- w_b — belt weight per unit length
- X, Y — factors in feeder load equations, flow condition
- y_e — depth of bulk solid in skirtplate zone, extended section
- y_h — depth of bulk solid in skirtplate zone, hopper section
- z — depth coordinates in hopper
- α — hopper half-angle
- β — angle in Eq. (17)
- γ — bulk specific weight

Mr. K.S. Manjunath, Graduate Research Student, and Dr. A.W. Roberts, Professor, Head of Dept. and Dean of the Faculty of Engineering, University of Newcastle, Dept. of Mechanical Engineering, Newcastle, N.S.W. 2308, Australia

δ — effective angle of internal friction
η — drive efficiency
μ — coefficient of friction
μ_2 — skirtplate friction coefficient
μ_b — belt idler friction
μ_i — coefficient of friction for bulk solid at feeder outlet
ξ — release angle
ϱ — bulk density
σ_1 — major consolidating pressure
σ_w — normal wall pressure
ϕ — wall friction angle.

1. Introduction

Feeders are used to provide a means of control for the withdrawal of bulk solids from storage units such as bins, bunkers, silos and hoppers. This control function can only be performed properly as long as the bulk solids flow by gravity to the feeders in a uniform and uninterrupted fashion. Feeders must be considered as an integral part of the overall bin and feeder system. Improper design of either one of these components will affect the performance of the whole system. The integrated concept of bin and feeder design requires analysis of the bulk solid characteristics before design and selection of the components can be attempted.

During the past few years, various papers have been presented on feeders and their applications. One of the problems encountered when using the Jenike approach [1] is the absence of an analytical expression for the surcharge factor determination. Results of numerical solutions are presented by Jenike [1] in chart form. McLean and Arnold [10] have presented an analytical expression for dimensionless surcharge factors using the Jenike theory. The purpose of the present paper is to discuss briefly the principles of feeder design, highlighting the determination of feeder loads and power requirements. Since feeder loads are influenced by the degree of support provided by the bin walls, this support being related to the wall pressure generated, a brief review of the wall pressures in mass flow bin is given. Further, the theory is substantiated by experimental investigation using a model plane flow bin and belt feeder, and a design example is included to illustrate the application to a hopper feeding bulk solids onto a belt feeder fitted with skirtplates.

2. Basic Design Considerations

2.1 Feeder Loads — General Remarks

Fig. 1 shows the loads acting in hopper and feeder. Feeder loads are influenced by factors such as:

- hopper flow pattern, whether mass flow or funnel flow
- flow properties of bulk solid
- the chosen hopper shape, which in the case of mass flow includes axisymmetric or conical, plane flow or transition (combination of conical and plane flow)
- the actual hopper geometry
- the wall friction characteristics between the bulk solid and hopper walls and skirtplates
- the type of feeder and its geometrical proportions
- the initial filling conditions when the bin is filled from empty condition and the flow condition when discharge has occurred.

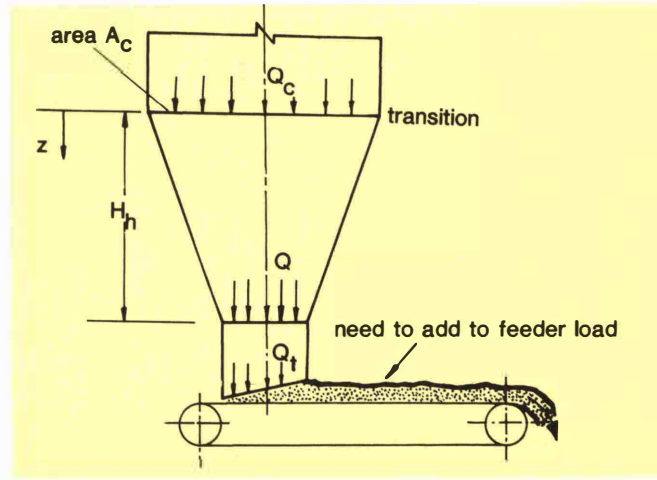

Fig. 1: Feeder loads in hopper/feeder combination

2.2 Hopper/Feeder Combination

In a hopper/feeder combination, the flow pattern should be such that the whole outlet of the feed hopper is fully active. In the case of wedge-shaped hoppers, to maintain a fully active outlet requires the capacity of the feeder to increase in the direction of feed. This may be achieved by using a tapered outlet [13]. Fig. 2 shows possible examples of a poor feeder with improperly adjusted control gates and vertical skirts. Gates should only be used as flow trimming devices and not as flow rate controllers. Flow rate control is achieved by varying the feeder speed.

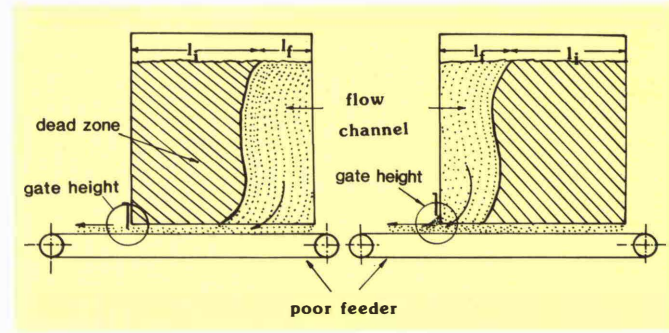

Fig. 2: Eccentric flow patterns in hopper/feeder combinations caused by incorrect gate setting

3. Model Plane Flow Bin and Belt Feeder

Experiments were conducted using a model variable geometry perspex plane flow bin and flat-bed-type feeder, as shown in Fig. 3. The bottom of the hopper is tapered in the direction of feed to assist in obtaining uniform draw [13]. The trimming of the flow is achieved by an adjustable gate. The belt feeder is suspended on vertical wires attached to load beams to permit the measurement of feeder loads. Horizontal restraining wires also attached to the load beams permit the measurement of tangential force to shear the bulk solid along the feeder. The vertical support wires are adjustable, making it possible to set the feeder at a chosen inclination or declination or even move the feeder relatively to the hopper outlet downwards or upwards, thereby controlling the clearance. The bin is filled from a chute either directly or via a distributer.

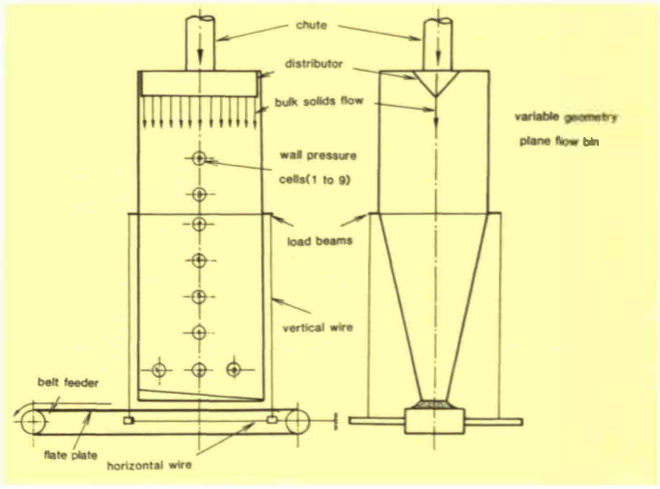

Fig. 3: Model variable geometry plane flow bin and belt feeder test rig

Nine pressure cells are accurately fitted in the positions shown in Fig. 3. These pressure cells are of the type described by Askegaard [17]. The deflection of the front plate under air pressure can be neglected. Three pressure cells along the outlet help to monitor the loads in the vicinity of the hopper outlet. Continuous pressure measurements have been recorded for both initial and flow loadings. The effects of belt speed, gate height, clearance between the hopper outlet and the feeder surface, type of filling, rate of filling on wall pressure distributions and feeder load and power requirements have been investigated, using plastic pellets and sand with different moisture content ranges.

3.1 Wall Pressure Measurement

Continuous traces of wall pressures for sand measured by eight pressure cells at different levels in the plane flow bin, which are typical of those found on many runs, are shown in Fig. 4. The pressures are shown to have built up smoothly during initial filling and to a higher level on the lower pressure cell. As soon as flow started, the readings from the pressure cells started to fluctuate. Flow pressures in the region just below the transition built up rapidly to levels substantially above the static values. During flow, stick-slip motion of the sand was observed. It should also be noted from Fig. 4 that, as soon as the flow was started, a transient overpressure occurred at each level of the pressure cell, moving rapidly up and locking at the transition. Once the time of this overpressure is known, it is possible to calculate the velocity of the switch wave. During stop/start, the dynamic pressure pattern remains unchanged.

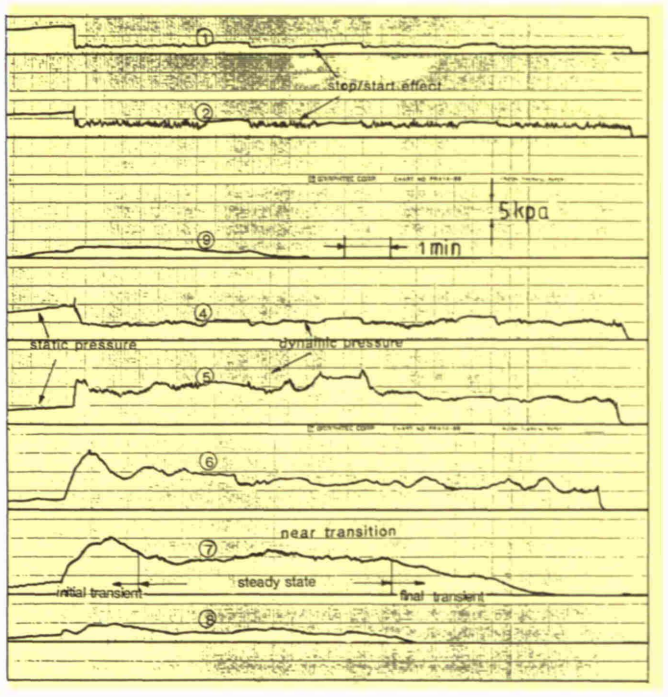

Fig. 4: Normal wall pressure recordings — bin: D = 0.53 m, B = 0.08 m, H = 0.63 m; material: δ = 33 °, ϕ = 20 °, ϱ = 1.52 t/m³

3.2 Feeder Load Measurement

Typical feeder load filling and emptying curves are presented in Fig. 5. The variation between initial filling and flow load is quite significant. Further, it is important to know that, once the flow has been initiated and the feeder stopped, the load on the feeder does not revert to the original initial load, but remains substantially the same as Q_f.

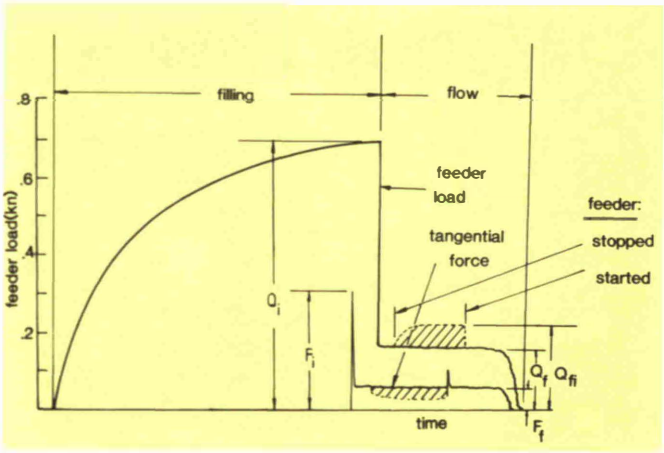

Fig. 5: Feeder load variations for plane flow bin and belt feeder test rig — bin: D = 0.53 m, B = 0.08 m, H = 0.63 m, L = 0.69 m, α = 14.5 °; material: white sand, δ = 33 °, ϕ = 20 °, ϱ = 1.52 t/m³

4. Pressure Distribution in Mass Flow Bins

In hopper/feeder combinations, the loads acting on the feeders are related to the pressures acting in mass flow hoppers. Fig. 6 shows the bin stress fields and corresponding pressure distribution for the initial filling (static) and flow (dynamic) cases. In each case, p_n represents the pressure acting normal to the wall, while p_v represents the average vertical pressure.

4.1 Pressure Distributions

4.1.1 Initial Filling Case

In this case (Fig. 6a), vertical support is provided and the major consolidating principal pressure is nearly vertical. A peaked/active stress field exists in both cylinder and hopper, as indicated. In the cylindrical part of the bin, the bulk solid contracts vertically only and a plastic-active state of pressure develops. The pressures in the cylinder are computed using the Janssen equation. In the hopper, an elastic-active state of pressure develops.

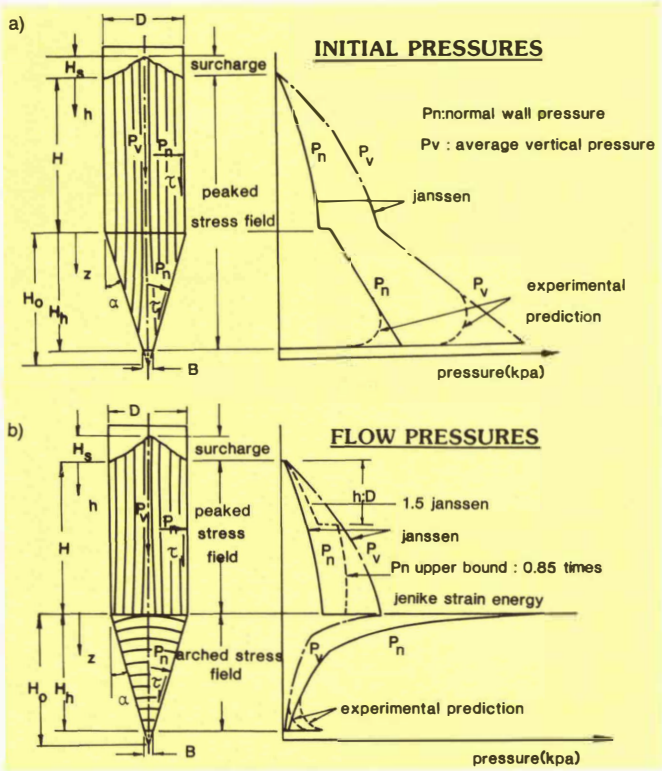

Fig. 6: Pressure distribution in mass flow bin

4.1.2 Flow Case

In this case (Fig. 6b), with the vertical support removed, the load is transferred to the hopper walls and the peaked stress field switches to an arched/passive stress field. During this state, the bulk solid contracts horizontally and expands vertically in the hopper. The major principal stress is almost horizontal, and a plastic-passive state of pressure exists. As flow is initiated from the hopper, the switching from a peaked to an arched stress field commences at the hopper outlet and travels upwards. There is evidence [1], [25] to suggest that the switch becomes locked at the transition and remains unchanged during continuous flow. During the flow, the peaked stress field remains in the cylinder, and for a perfectly parallel cylinder without localised convergences, the Janssen stress field remains. However, in practice, localised convergences are difficult to avoid, such convergences being caused by weld projections or shrinkages in the case of steel bins. For this reason, an upper bound normal wall pressure based on Jenike's strain energy stress field [25] is computed for design purposes. The modified upper bound cylinder normal wall pressures are shown in Fig. 6.

4.2 Hopper Pressures [23], [26]

For the determination of feeder loads, the pressure acting in mass flow hoppers requires examination. The normal pressure p_n is related to the average vertical pressure p_v by a parameter K such that

$$K = \frac{p_n}{p_v} \tag{1}$$

From an equilibrium analysis the following equation is obtained:

$$p_n = \gamma K \left[\frac{h_o - z}{n-1} + \left(h_c - \frac{h_o}{n-1} \right) \left(\frac{h_o - z}{h_o} \right)^n \right] \tag{2}$$

where:

$$n = (m+1) \left[K \left(1 + \frac{\tan\phi}{\tan\alpha} \right) - 1 \right] \tag{3}$$

where:

μ — coefficient of wall friction; $\mu = \tan\phi$
ϕ — wall friction angle.

h_c follows directly from the Janssen equation, being given by:

$$h_c = \frac{R}{\mu K_j} \left(1 - e^{-\mu K_j H/R} \right) + h_s e^{-\mu K_j H/R} \tag{4}$$

where:

H — height of material in contact with cylinder walls
R — hydraulic radius;

$$R = \frac{D}{2\,(1+m_c)} \tag{5}$$

m — cylinder shape factor; $m_c = 0$ for long rectangular cylinder, $m_c = 1$ for square or circular cylinder
K_j — pressure ratio; $K_j = p_n/p_v$ for cylinder.

The value of K_j varies depending on the cylinder geometry. For parallel sided cylinders with slight convergences, Jenike suggests:

$$K_j = 0.4 \tag{6}$$

For continuously diverging or stepwise diverging cylinders without convergences, the theoretical value of K_j may be used:

$$K_j = \frac{1 - \sin\delta}{1 + \sin\delta} \tag{7}$$

where:

δ — effective angle of internal friction for the bulk solid.

For continuously converging cylinders, K_j is approximated by:

$$K_j = 1 \tag{8}$$

h_s in Eq. (4), representing the surcharge acting on the top surface of the bin, depends on the way the bin is loaded. Assuming central loading, then for the axisymmetric bin a conical surcharge is assumed; for a plane flow bin in which the length is greater than the width, an approximate triangular shape would occur if a travelling feeding device such as a tripper is used. With these two limits:

$$h_s = \frac{H_s}{m_s + 2} \tag{9}$$

where:

m_s — surcharge factor; $m_s = 0$ for triangular surcharge, $m_s = 1$ for conical surcharge
H_s — actual surcharge.

For a plane flow bin, some rounding of the ends of the top surface of the bulk material is likely to occur so that an approximate intermediate value of m_s can be used.

4.2.1 Initial Filling Case

For the initial filling condition in the hopper, Jenike [23] assumes that the average vertical pressure distribution in the hopper follows the linear hydrostatic pressure distribution. For this condition, the value of K in Eq. (2) is the minimum value. That is:

$$K = K_{min} = \frac{\tan\alpha}{\tan\phi + \tan\alpha} \quad (10)$$

where:

ϕ — wall friction angle for the hopper.

Substitution into Eq. (3) yields $n = 0$.

$$p_n = \gamma K_{min} (h_c + z) \quad (11)$$

and:

$$p_v = \frac{p_n}{K_{min}} = \gamma (h_c + z) \quad (12)$$

The linear relationships for p_n and p_v for the hopper are shown in Fig. 6a.

The dotted line in Fig. 6a shows the experimental values of the normal wall stress p_n and the average vertical stress p_v. In the vicinity of the outlet, both the pressures are nonlinear and curve inward away from the hydrostatic pressure. This is primarily due to the clearance between the feeder and the hopper outlet and the rigidity of the skirt zone. The bulk solid in the interfacial zone provides a certain degree of cushioning. Therefore, the measured values of n and K for initial filling are less than the theoretical values; they are discussed in Section 5.

4.2.2 Flow Case

In this case, the vertical gate support is removed, the load is transferred to the hopper walls and the peaked stress field switches to an arched stress field. As flow is initiated, the switching from a peaked to an arched stress field commences at the hopper outlet and travels upward. There is evidence to suggest that the switch becomes locked at the transition and remains there during continuous flow. Even when flow is stopped, the arched stress field remains. In the arched stress field, the major principal stress acts more in the horizontal direction.

The normal wall pressures for flow in the hopper are given by Eq. (2), with K set at the maximum value:

$$K = K_{max} \quad (13)$$

where K_{max} is given in graphical form in Ref. [23] or else may be computed using equations derived in Ref. [11]. These are:

$$K_{max} = \frac{\sigma_w}{\gamma B} / q \left(\frac{4}{\pi}\right)^m \quad (14)$$

where:

$$\frac{\sigma_w}{\gamma B} = \frac{Y (1 + \sin\delta \cos 2\beta)}{2 (X - 1) \sin\alpha} \quad (15)$$

and:

$$q = \left(\frac{\pi}{3}\right)^m \frac{1}{4 \tan\alpha} \left[2 \frac{\sigma_w}{\gamma B} (\tan\alpha + \tan\phi) - \frac{1}{1+m}\right] \quad (16)$$

where:

$$\beta = \frac{1}{2}\left[\phi + \sin^{-1}\left(\frac{\sin\phi}{\sin\delta}\right)\right] \quad (17)$$

$$X = \frac{2^m \sin\delta}{1 - \sin\delta}\left[\frac{\sin(2\beta + \alpha)}{\sin\alpha} + 1\right] \quad (18)$$

$$Y = \frac{\{2[1 - \cos(\beta + \alpha)]\}^m (\beta + \alpha)^{1-m} \sin\alpha + \sin\beta \sin^{1+m}(\beta + \alpha)}{(1 - \sin\delta) \sin^{2+m}(\beta + \alpha)} \quad (19)$$

where:

ϕ — wall pressure angle; $\phi = \tan^{-1}\mu$
δ — effective angle of internal friction
m — hopper shape factor; $m = 1$ for axisymmetric flow or conical hopper, $m = 0$ for plane flow or wedge-shaped hopper.

In Eq. (19) in the numerator term $(\beta + \alpha)^{1-m}$, both β and α must be in radians.

The dotted line in Fig. 6b shows the experimental curve for the flow case. The measured normal wall pressures deviate slightly from the radial stress field line. Therefore, the dynamic load on the feeder is much higher than predicted from the radial stress field theory of Jenike [25]. The measured value of n is less than the computed value.

4.3 The Switch Stress Field in the Hopper

When the hopper is initially filled, a peaked stress field exists in the hopper. During withdrawal of the bulk solid, the state of stress changes to an arched stress field. This is essentially instigated by a transient overpressure at the outlet of the hopper and travels up through the bulk solids in the form of stress disturbance. Let us suppose that at some instant the disturbance has reached the dimensionless depth Zh below the transition, as shown in Fig. 7. We will assume that above

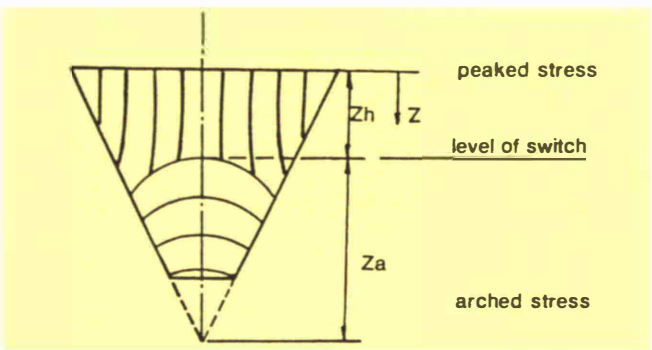

Fig. 7: Stress fields in a hopper

the switch stress field there is still the undisturbed peaked stress field described by Eq. (2), with static values of n and K. Below the switch there is the arched stress field given by Eq. (2), with a dynamic value of K. The envelope of this switch stress field is given by:

$$(p_s)_{en} = \frac{K_{max}}{K_{min}} (p_n)_s \quad (20)$$

The switch stress envelope normal to the wall is thus (K_{max}/K_{min}) times the static normal wall stress $(p_n)_s$.

5. Influence of K and n on the Wall Pressure Distributions

The experimental feeder loads during initial filling are generally less than the theoretical values, although the upper bound for initial filling is characterised by $n = 0$ in the foregoing analysis. This is due to the minimum value of K, K_{min}, which results in hydrostatic pressure distributions. Furthermore, in the analysis both n and K are assumed to be constant for each section of the hopper for each of the initial and flow situations. Hence it is interesting to examine the sensitivity of hopper pressure distributions to the variations in the value of n.

As is seen from Fig. 8, a slight variation in the positive value of n results in a significant reduction of the average vertical pressure p_v, which is of particular importance as far as feeder loads are concerned. The numbers in parentheses in Fig. 8 represent the values of K. For the determination of hopper wall loads, the influence of the variation of n on the normal wall pressure p_n is required. Fig. 8 applies to the hopper section only for a surcharge head of 0.63 m in the cylinder. The theoretical value of $n = 0$ for the initial filling case corresponds to a value of $K_{min} = 0.415$. For the flow case, $K_{max} = 2.17$, corresponding to $n = 4.23$. The hatched area to the right in Fig. 8 corresponds to the experimental determination of the range of values of K during initial filling and that to the left to that during flow. The negative values of n, as shown, lead to large values of vertical loads. Following Walters [16], it can be shown that the hopper half-angle α must be less than $(\pi/2 - \epsilon_1)$ for a fully active fill condition to develop. If α exceeds the limit, it seems doubtful whether an active state of stress can exist throughout the hopper.

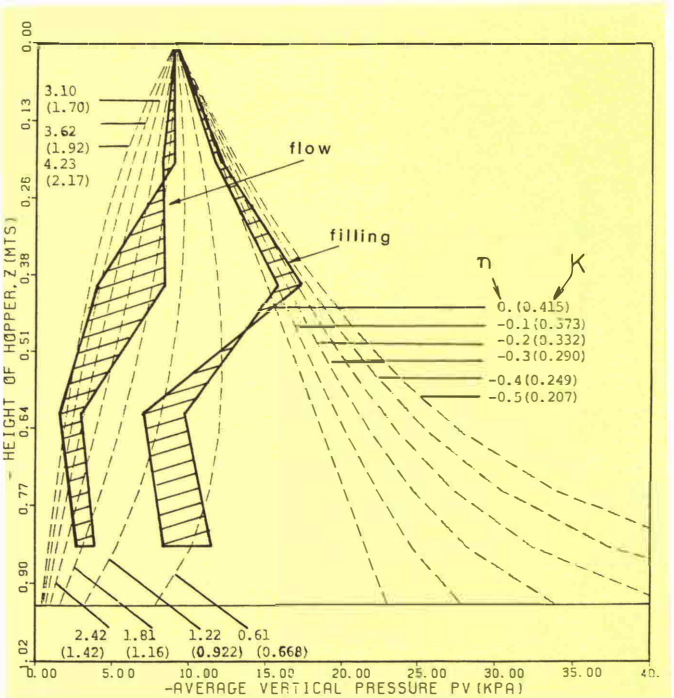

Fig. 8: Average vertical pressures based on Eqs. (1) and (2) acting in the hopper for a plane flow bin and belt feeder test rig — bin: $D = 0.53$ m, $B = 0.08$ m, $H = 0.63$ m, $L = 0.69$ m, $\alpha = 14.5°$; material: white sand, $\delta = 33°$, $\phi = 20°$, $\varrho = 1.52$ t/m³

6. Theoretical Prediction of Feeder Loads and Power

The theoretical prediction of the surcharge load acting at the outlet of a mass flow hopper requires consideration of both the initial and flow consolidation pressures acting on the bulk solid.

6.1 Generalised Expression for the Nondimensional Surcharge Factor

To evaluate the loads imposed on feeders and the peak stress on the wall at the transition of a mass flow bin requires the evaluation of the resultant vertical force across a horizontal cross section of a mass flow hopper. This force is evaluated in terms of a dimensionless number called the surcharge factor q.

According to McLean and Arnold [10], the surcharge Q acting at the outlet of the hopper is given by:

$$Q = q\,\gamma\,L^{1-m}\,B^{m+2} \qquad (21)$$

The surcharge Q is the product of the average vertical pressure p_{vo} at the outlet and the area of the outlet. This leads to the expression:

$$Q = p_{vo}\,(\pi/4)^m\,L^{1-m}\,B^{m+1} \qquad (22)$$

The nondimensional surcharge factor q from the above equations is given by:

$$q = (\pi/4)^m\,p_{vo}/\gamma B \qquad (23)$$

Hence a generalised expression for the nondimensional surcharge factor q may be derived. Following Roberts et al. [26]:

$$q = (\pi/4)^m\,\frac{1}{2(n-1)\tan\alpha}\left\{1 + [2(n-1)\,h_c\tan\alpha - D]\,\frac{B^{n-1}}{D^n}\right\} \qquad (24)$$

Eq. (24) may be used to compute q, provided the pressure ratio K and hence the value of n for the prevailing pressure conditions are known at the outlet. Often the actual value of n is not known, particularly when there is a reasonable clearance between the hopper outlet and the feeder. In such cases, a discontinuity in pressure distribution at the outlet leads to some uncertainty as to the validity of the Eq. (24). Some elaboration of this matter is provided in the analysis and discussion in Sections 5. and 7.

6.2 Special Cases

For the design purposes, the surcharge factors and hence feeder loads are required for two conditions:

— initial filling
— flow.

6.2.1 *Nondimensional Surcharge Factor q_i for Initial Filling Conditions*

The determination of the initial feeder surcharge factor requires the consideration of the initial wall loads acting on the hopper walls. As reported by Roberts et al. [26], assuming the initial pressure distribution as hydrostatic in form, for which $n = 0$ and $K = K_{min}$, then the substitution of $n = 0$ in Eq. (24) yields:

$$q_i = (\pi/4)^m \frac{1}{2\tan\alpha}\left(\frac{D}{B} + \frac{2\,h_c\tan\alpha}{B} - 1\right) \quad (25)$$

By way of comparison, McLean and Arnold [10] have derived an expression for the initial surcharge factor q_i based on the original Jenike theory [25]. They determined the surcharge at the outlet from an equilibrium analysis, taking into account the weight of the material in the hopper section, the surcharge at the transition and the vertical support provided by the hopper walls. The expression is:

$$q_i = (\pi/4)^m \frac{1}{2\tan\alpha}\left(\frac{D}{B} + \frac{2\,h_c\tan\alpha}{D} - 1\right) \quad (26)$$

It will be noted that Eqs. (25) and (26) are identical except for the denominator of the middle term of the section contained within the second parentheses; in Eq. (25) the denominator includes B, while in Eq. (26) it is D. Both equations give identical results for the case of a hopper without surcharge, i.e., $h_c = 0$; otherwise Eq. (25) leads to higher values of q_i than does Eq. (26).

Experimental evidence to date suggests that Eq. (26) gives satisfactory prediction of the initial surcharge factor, although in some cases the predictions are slightly conservative. Eq. (25) may be approached in the case of a flat plate held firmly against the bottom of the rigid hopper. However, in the case of a feeder, there is usually a reasonable clearance and/or skirtplates which induce an initial flow stress field in the region of the outlet, and this has the effect of providing some cushioning of the initial load. Eq. (25) is regarded as an upper bound solution.

6.2.2 Nondimensional Surcharge Factor q_f during Flow

Following McLean and Arnold [10], the flow nondimensional surcharge factor is given directly by Eq. (16). Substituting for $\sigma_w/\gamma B$ from Eq. (15) into Eq. (16) gives:

$$q_f = \frac{1}{4}\left(\frac{\pi}{3}\right)^m \frac{1}{\tan\alpha}\left[\frac{Y}{X-1}\left(\frac{1+\sin\alpha\cos 2\beta}{\sin\alpha}\right)(\tan\alpha+\tan\phi) - \frac{1}{1+m}\right] \quad (27)$$

where β, X and Y are given by Eqs. (17), (18) and (19), respectively.

Charts for q_f are also presented in Ref. [11].

Experimental evidence [26] suggests that feeder loads during flow based on the nondimensional surcharge factor q_f given by Eq. (27) are underestimated. The same evidence also suggests that a more realistic estimate of the feeder load is obtained by using a method based on that due to Roberts et al. [26]. This is described in the following section.

6.3 Recommended Flow Loads

Reisner has proposed two methods for determining the loads on feeders during flow, these methods being based on the assumption that the stress field shifts and rotates above the feeder, causing a different vertical stress. In one case, he suggests that for belt, apron and table feeders the load acting on the feeder be computed on the basis of the pressure σ_w which acts normal to the hopper wall. In the other case, he has proposed that for vibratory feeders the load be determined on the basis of the major consolidation pressure σ_1. Recent research [26] suggests that the flow loads for belt feeders also be determined on the basis of the major consolidation pressure σ_1; σ_1 is assumed to act downward at the outlet. σ_1 is given by:

$$\sigma_1 = \frac{\gamma B ff}{H(\alpha)} \quad (28)$$

where:

γ — bulk specific weight
B — diameter or width of outlet
ff — flow factor
$H(\alpha)$ — function of hopper half-angle α; depends on the shape of the hopper opening.

Charts for the flow factor ff and function $H(\alpha)$ are given in Ref. [11].

Putting $p_{vo} = \sigma_1$ and substituting expressions for ff and $H(\alpha)$ from Ref. [11] into Eq. (28), then from Eq. (22) the nondimensional flow surcharge factor may be derived:

$$q_{f\sigma_1} = \left(\frac{\pi}{4}\right)^m \frac{Y(1+\sin\delta)}{2(X-1)\sin\alpha} \quad (29)$$

where:

α — hopper half-angle
δ — effective angle of internal friction.

X and Y are given by Eqs. (18) and (19), respectively.

As has been shown by Roberts et al. [26], Eq. (29) provides a better prediction of the flow surcharge factor than does Eq. (27). It also has the advantage of being a less cumbersome expression. It is recommended that Eq. (29) be used.

Part II of this article will follow in issue No. 5, October 1986 (Focus: Scandinavia). It will contain the following main Chapters:

7. Experimental Results and Discussion
8. Power to Shear Bulk Solid in Hopper
9. Influence of Hopper Geometry on Feeder Loads
10. Controlling the Feeder Loads
11. Effect of Hopper Wall Rigidity on Feeder Design
12. Total Power Requirements for Belt Feeders
13. Summary of Conclusions.

The List of References will follow in Part II.